Separation of the surface and bulk recombination in silicon by means of transient photoluminescence

Friedemann D. Heinz,[a] Wilhelm Warta, and Martin C. Schubert
Fraunhofer ISE, Heidenhofstr. 2, 79110 Freiburg, Germany

(Received 15 December 2016; accepted 16 January 2017; published online 25 January 2017)

The bulk and surface recombination determine the electrical performance of many semiconductor devices. Yet, the experimental determination and separation of both surface and bulk recombination rate remains challenging. This paper presents the measurement and separation of the bulk and surface recombination in silicon by means of time resolved photoluminescence spectroscopy. The high temporal resolution of the applied time correlated single photon counting technique is exploited to access the photoluminescence response of a silicon sample upon pulsed excitation in the nanosecond to millisecond regime on a sub-cm^2 area. A rigorous data fitting algorithm based on two dimensional numeric simulations of the induced charge carrier dynamics is applied to extract all information on bulk and surface recombination properties from the recorded photoluminescence transients. Using different samples with symmetric as well as asymmetric surface recombination properties, we demonstrate the capabilities of the proposed contactless and nondestructive technique, which may be applicable to silicon based mono- or multi-junction devices. *Published by AIP Publishing.* [http://dx.doi.org/10.1063/1.4975059]

The bulk and surface recombination of minority carriers determine the electrical performance of many semiconductor devices.[1] The recombination properties depend on the doping density, processing, surface treatment, and has to be characterized for optimization of the electric device performance. For example, in photovoltaics, the ideal charge carrier lifetime, which ensures a high conversion efficiency, depends on the cell architecture,[2] which implies that both bulk and surface recombination must be optimized and hence be measured.

In principle there are two approaches for separating the bulk and surface recombination, (1) measurement of the depth profile of the charge carrier density Δn in steady state (recombination at the sample surfaces leads to a convex Δn profile) or (2) measurement of the transient evolution of the decay of Δn measured integrally over the sample depth upon an excitation pulse (recombination at the surface leads to a fast initial decay of Δn).

The immediate realization of approach (1) has up to now not been realized, as a depth selective determination of Δn with high spatial resolution is difficult. Yet, different workarounds were proposed to obtain the depth information on Δn: The entire depth profile must not be known, but rather the information on Δn from at least two sample depths. This can be done exploiting the reabsorption of luminescence within the sample. Using edge filters, electroluminescenc[3] or PL[4] from different sample depths can be measured. Baek *et al.* use different excitation wavelengths to generate different Δn profiles.[5] Furthermore, asymmetric samples were used in combination with measurements from a reference sample[6] or by combining measurements from both sides of the sample.[7] A drawback of these techniques is the necessity to compare the intensity of at least two independent measurements, which may lead to systematic experimental errors: The differences between these measurements need to be known exactly (e.g., filter parameters and possible changes in optics due to additional filters and surface morphologies).

The separation of bulk and surface recombination within *one* measurement may be reached using approach (2). Both recombination channels may be determined uniquely from the transient Δn decay due to their different influence at different decay times: In the presence of surface recombination, fast decay modes increase the total recombination rate (i.e., a fast decrease of PL intensity) for decay times up to about 1 μs until the surface near region is depleted of minority charge carriers whereas the asymptotic decay, which quantifies the effective lifetime, is determined by both surface and bulk recombination. This effect was described quantitatively by Luke and Cheng in 1987.[8] Their theoretical analysis of the average charge carrier density decay led to a semi-analytic expression separating the "effective" lifetime τ_{eff} into the bulk lifetime τ_b and an infinite number of surface recombination dependent decay modes. While their analysis promised a sensitive approach, their experimental capabilities could not provide sufficient accuracy: Recording the fast transient decay (within some μs) of the charge carrier density in the presence of surface recombination requires a high temporal resolution of the apparatus. In the following decade, their concept of decay modes was adapted to several experiments based on photoconductance,[9,10] free carrier absorption,[11–13] reflectance,[14] induced current,[15] the open circuit voltage[16] and was extended for samples asymmetric with respect to the surface recombination velocity (SRV).[12,13] Thereby, methods based on two wavelength excitation (e.g., in Ref. 9) suffer from uncertainties of the normalization of the exponential decays.

A satisfactory experimental realization of the detection of the transient charge carrier decay could up to now not be

[a]Author to whom correspondence should be addressed. Electronic mail: friedemann.heinz@ise.fraunhofer.de

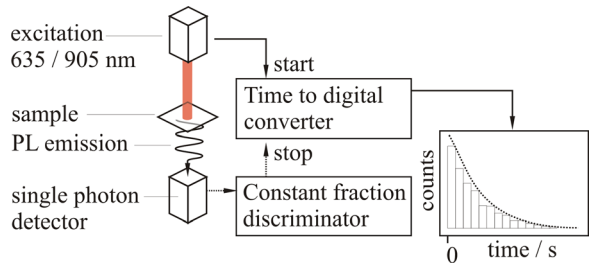

FIG. 1. Experimental setup for recording the transient PL evolution with a high temporal resolution.

achieved "owing to the unavoidable measurement noise and on *non-perfect linearity* of measurement systems."[17] Non-linearities yield a disadvantage in particular, to all techniques measuring the microwave reflectance or transmission.[18] In this paper we evaluate the transient decay of Δn in silicon by means of a *detection of the PL emission*. This reveals key improvements compared to all approaches available up to now: Non-linearities of PL as a probe of Δn are well understood and may be quantified.[19]

Furthermore, all present methods which obtain the SRV from a transient Δn decay are based on the analysis of Luke and Cheng,[8] which aims for a suitable *data reduction* which inevitably leads to either an amplification of noise (e.g., when fitting only few data points to obtain the initial decay rate) or a loss of information and hence a decrease of sensitivity. Due to the accuracy of present numeric approaches for the purpose of solving the equation of continuity of Δn (Ref. 19) we do not necessitate the use of the semi-analytic expressions derived by Luke and Cheng[8] and implement a rigorous data fitting routine and a statistical error estimation based on numeric simulations.

In the following, the capabilities and limitations of the presented approach based on the time resolved detection of the PL emission and numeric evaluation using different symmetric and asymmetric samples (different front and back surface recombination) are evaluated.

The experimental setup depicted in Figure 1 is based on time correlated single photon counting resulting, in our case, in a temporal resolution below 100 ps. Pulsed laser excitation is realized with diode lasers with wavelengths of 640 or 905 nm, respectively. The pulse duration is 0.5 ns, the half width of the Gaussian laser spot on the sample surface is 831 μm. Emitted photons are detected in transmission with an ultra-low noise photomultiplier tube operating in the Geiger mode (dark count rate (4.1 ± 0.1) cps) with a constant QE of 2.2% in the range of 950–1160 nm. Attenuation of spurious laser light incident on the photomultiplier tube (PMT) is done with a stack of a silicon filter with anti-reflection coating optimized at 1150 nm and a dielectric edge filter with a cutoff wavelength at 1000 nm. With this setup, a maximum injection level of $10^{13}\,\mathrm{cm}^{-3}$ is reached with a single laser pulse.

In order to quantify the PL intensity transients, the equation of continuity in two dimensions (radial symmetry $\mathbf{r} = (r, z)$) is solved numerically using a finite elements approach. The equation of continuity solved reads

$$\frac{\partial \Delta n}{\partial t} - \nabla(D(\Delta n)\nabla(\Delta n)) = -\Delta n\left(\frac{1}{\tau_\mathrm{b}} + \frac{1}{\tau_\mathrm{intr}}\right) + G, \quad (1)$$

$$-D(\Delta n)\mathbf{n}\nabla(\Delta n)|_{z=0} = S_\mathrm{front}\Delta n,$$
$$-D(\Delta n)\mathbf{n}\nabla(\Delta n)|_{z=W} = S_\mathrm{back}\Delta n \quad (2)$$

with normal vector $\mathbf{n}$, sample thickness W, ambipolar diffusion coefficient D modelled with Klaassen-Schindler's mobility,[20] defect bulk recombination lifetime τ_b, intrinsic bulk lifetime τ_intr accounting for radiative and Auger recombination, G the generation rate, and SRV $S_\mathrm{front/back}$ at the front and back surface of the wafer, respectively. The initial condition $\Delta n(\mathbf{r}, t = 0)$ for the transient case ($G = 0$) is determined by

- the photon flux of a single laser pulse deduced from the average laser power measured using a Newport Powermeter and the pulse distance,
- the reflectivity measured with a Lambda950 spectrometer,
- the Gaussian excitation spot size on the sample surface with a half width measured by scanning the cleaved edge of a silicon wafer (the intensity follows an error function),
- the absorption coefficient of silicon taken from Ref. 21.

In Figure 2(a), an exemplary mesh is depicted. Towards the surfaces, it is refined with a mesh size below the absorption depth of the laser light. Furthermore, this mesh is refined according to the gradients of a steady state $(\partial \Delta n/\partial t = 0)$ solution of the equation of continuity as shown in Figure

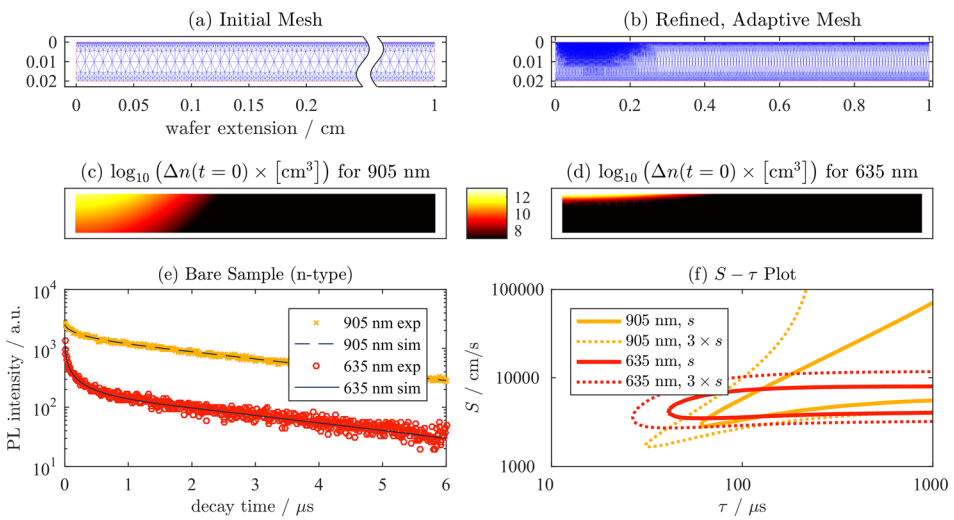

FIG. 2. (a) and (b) depict the initial mesh with a high mesh density at the surface (mesh size smaller than the laser penetration depth) and a refined adaptive mesh based on the gradient of a steady state solution of Eqs. (1) and (2) on a symmetry element. In (c) and (d), the injection level $\Delta n(\mathbf{r}, t = 0)$ (scaled identically) subsequent to the laser pulse are shown using a 905 and 635 nm excitation, respectively. (e) shows the measured (symbols) and fitted the PL decays. In (f) $S - \tau$ plots are shown. The enclosed areas indicate the value pairs within one or three standard deviations s distance of the best fit.

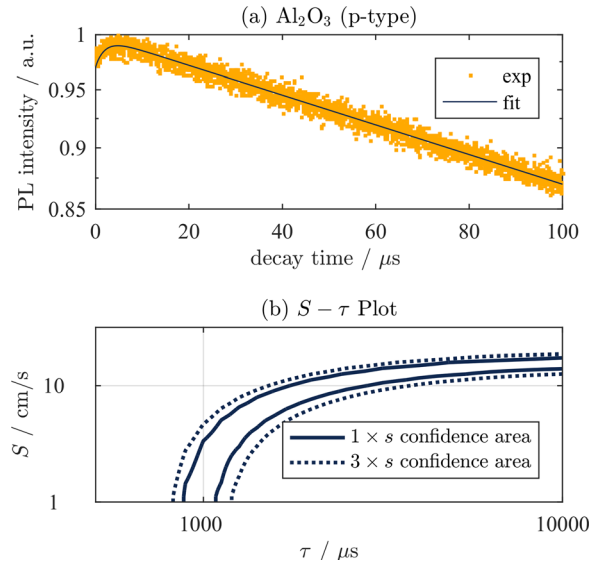

FIG. 3. (a) Measurement (symbols) and fit of the PL decay of an Al_2O_3 passivated sample. In (b), the $S - \tau_b$ plot shows the value pairs which are located within one or three standard deviations from the ideal fit.

2(b). Figures 2(c) and 2(d) depict the initial Δn distribution when using 905 nm (c) or 635 nm excitation (d) for a typical excitation power confirming the assumed low level injection (LLI) condition. LLI conditions ensure an injection independent charge carrier lifetime, yet, the SRV may be injection dependent.[22] From the measurements (cf. Figures 2(e), 3(a), and 4(a)) it can be seen that about one order of magnitude of injection level (PL intensity $\sim \Delta n$ at LLI) is covered within one measurement, we thus obtain an SRV averaged over this injection level range (typically 10^{12}–$10^{13}\,\mathrm{cm}^{-3}$). The injection dependence of the SRV needs also to be considered when applying the results to highly efficient solar cell devices operating at high injection conditions up to 10^{15}–$10^{16}\,\mathrm{cm}^{-3}$.

From the numeric solution $\Delta n = \Delta n(\mathbf{r}, t)$ of the transient equation of continuity, the measurable PL intensity $I_{\mathrm{calc}}(t)$ is calculated via

$$I_{\mathrm{calc}}(t) = \mathrm{c} \int_0^\infty QE(\lambda) \int_V p(\mathbf{r}, \lambda) B(\Delta n, n_0) \Delta n(\Delta n + n_0)\, \mathrm{d}\mathbf{r}\mathrm{d}\lambda. \tag{3}$$

B is the coefficient of radiative recombination, n_0 is the concentration of ionized dopants, $p(\mathbf{r}, \lambda) = p(z, \lambda)$ describes the probability for the reabsorption of emitted PL of wavelength λ and $QE(\lambda)$ the quantum efficiency of the setup determined by the known QE of the PMT and the filters. The parameters, $p(z, \lambda)$ and $QE(\lambda)$, need to be accounted for, in order to obtain reliable results, as the contribution of reabsorption is a function of time (due to depth diffusion). All effects of intensity weighting[23] are accounted for by the simulation. Knowledge of the external quantum efficiency c is not required as the injection level is deduced from the photon flux of the excitation pulse. Details and a verification of the finite elements approach are described elsewhere.[19]

For a quantitative evaluation of the measured transient PL evolution $I_{\mathrm{exp}}(t_i)$, the reduced χ^2 expression

$$\chi^2_{\mathrm{red}}(c, S, \tau_b) = \frac{1}{N_{\mathrm{dof}}} \sum_{i=1}^{N} \frac{\left[I_{\mathrm{exp}}(t_i) - c \times I_{\mathrm{calc}}(t_i, S, \tau_b)\right]^2}{\sigma_i^2} \tag{4}$$

is minimized. t_i is the time stamp of the ith discrete time bin (10–40 ns) in the measurement (total number of time bins is N), $\sigma_i^2 = I_{\mathrm{exp}}(t_i)$ is the variance of the measured intensities in the case of single photon counting (Poisson statistics; strictly, χ^2 testing is valid only for normally distributed errors, yet, for count rates of above 30 per time bin, Poisson statistics approaches a normal distribution. This is fulfilled in experiment), $N_{\mathrm{dof}} = N - 3$ is the degrees of freedom. The standard deviation s of the minimum of χ^2_{red}, which is used as an error estimate (S – τ_b plots), is $s = \sqrt{2/N_{\mathrm{dof}}}$. The minimum of χ^2_{red} is gained using a simplex minimization method (Nelder-Mead[24]). In order to give an error estimate on S and τ_b, an algorithm is implemented which determines all (c, S, τ_b) parameter sets which result in a χ^2_{red} below s and $3 \times s$ which may be visualized using $S - \tau_b$ plots. The calculation of a single PL decay transient for one set of parameters (c, S, τ_b) takes about 5–30 s.

We investigate the different samples to demonstrate the sensitivity of the proposed procedure. In Figure 2(e), the measured PL (symbols) and fitted transients of a shiny etched 1 Ωcm n-type silicon sample (native oxide, effective lifetime $\tau_{\mathrm{eff}} = 3.5$ μs) excited with 635 and 905 nm wavelengths are shown. The fitted decay curves result in $\chi^2_{\mathrm{red,\,635}} = 1.49 \pm 0.06$ and $\chi^2_{\mathrm{red,\,905}} = 1.48 \pm 0.06$, respectively. Regarding the $S - \tau_b$ plots of χ^2_{red} in Figure 2(f), we obtain the SRV to be $> 2.2 \times 10^4$ cm/s (905 nm) and $(3.2 - 7.1) \times 10^4$ cm/s (635 nm) and a lower limit of the bulk lifetime of 40 μs. Please note the strong covariance of S and τ_b. The higher sensitivity for determining the SRV using a 635 nm excitation originates in the more shallow penetration depth of the laser light which leads to an increase of the recombination at the illuminated surface. Yet, the lower s/n

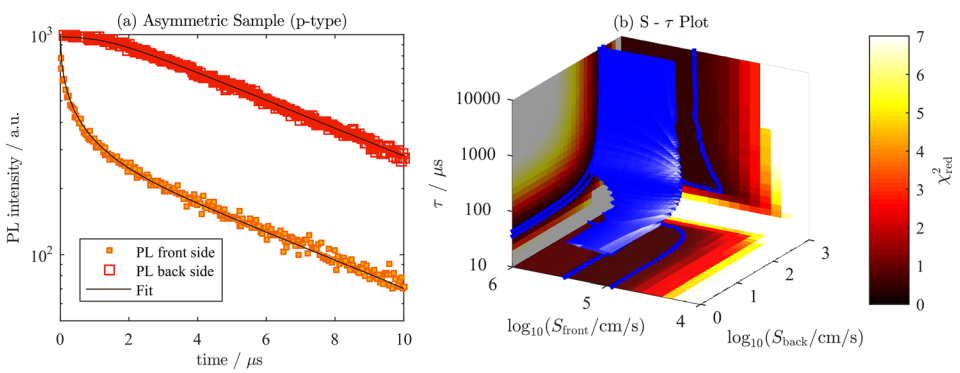

FIG. 4. Measured and simulated PL decay curve on a sample which is asymmetric with respect to the surface recombination velocity (a). In (b), the S–S–τ plot shows the confidence volume (blue) and its projections (the coarseness of the shining effect which is used to clarify the volume shape is caused by the discreteness of the simulated data).

ratio when using a 635 nm excitation due to the fast initial PL decay increases the experimental uncertainty, which explains the fact that the $S-\tau_b$ plot of this measurement is not entirely contained within the $S-\tau_b$ plot of the measurement with 905 nm excitation.

Figure 3(a) shows the measurement (symbols) and the fitted transient of an Al_2O_3 passivated *p*-type FZ wafer with protective SiN_x capping which is expected to exhibit a low SRV. Surprisingly, the PL intensity rises subsequent to the laser pulse. This can be understood considering an attenuation of reabsorption of PL due to diffusion of charge carriers from the illuminated surface into the sample depth towards the detector without a notable recombination (measurement in transmission). This effect is verified by the simulation as demonstrated in Figure 3(a). Due to the slow decay time, the s/n ratio is low which results in the rather low $\chi^2_{red} = 0.08 \pm 0.03$. From the $S-\tau_b$ plot in Figure 3(b), it can be stated that the bulk lifetime must be above 830 μs and $S < 15$ cm/s, which is the same information which can be retrieved from a lifetime measurement. This shows the experimental limit of the transient approach for very low surface recombination which does not cause significant recombination subsequent to the excitation pulse.

Finally, the proposed technique is applied to a sample with asymmetric front and back surface recombination. For this purpose, the transient PL intensity decay is measured from either side and both transients are fitted simultaneously using parameter sets $(c, S_{front}, S_{back}, \tau_b)$ and $N_{dof} = N_{front} + N_{back} - 4$. Figure 4(a) shows the transients measured (symbols) from either side of a 1 Ωcm *p*-type silicon sample which was passivated with a non-ideal Al_2O_3 layer from one side (effective lifetime $\tau_{eff} = 6.9\,\mu s$). We obtain $\chi^2_{red} = 0.26 \pm 0.03$ and from the volumetric $S_{front} - S_{back} - \tau_b$ plot in Figure 4(b), we deduce $S_{front} < 320$ cm/s and $S_{back} > 1.2 \times 10^5$ cm/s and $\tau_b > 39\,\mu s$. A strong covariance is visible, i.e., any further information or assumption on either of the three parameters would strongly tighten the confidence interval of the remaining parameters.

From the simulated decay curves assuming either surface or bulk limited lifetime, it is concluded that a separation of the surface and bulk recombination is possible for SRVs in the range 50–10^5 cm/s for typical doping densities and sample thicknesses. For lower or higher SRVs, a higher or lower border of the SRV can be given (cf. symmetric Al_2O_3 passivated sample). The technique is applicable to various sample geometries. Considering the small excitation area below 1 mm^2, single grains of mc silicon can be investigated. Long wavelength excitation with a 905 nm excitation may be used to investigate the silicon bottom cells in tandem devices with a large bandgap top cell like perovskites. Also, the recombination at localized structures on the surface which yield an axial symmetry may be investigated, e.g., local contacts or dislocations. The applicability of this technique to asymmetric samples may be exploited to investigate the fully processed solar cells to determine the effective front and back surface recombination velocity between two fingers and hence, e.g., the functioning of a back surface field, however requiring a simulation of emitter effects.

Summing up, we demonstrated the suitability of time correlated single photon counting to record the transient photoluminescence decay in silicon after pulsed excitation with high temporal resolution on small areas. The implementation of a two dimensional numeric simulation in combination with a full statistical analysis of the experimental PL decay curves allows for dropping all assumptions and approximations which needed to be done up to now in terms of data reduction as proposed by Luke and Cheng. Using different samples and a statistical data analysis, we demonstrated the sensitivity of this approach for determining the surface recombination velocity in the range of about 50 cm/s –10^5 cm/s. We showed the better s/n ratio when using a long excitation wavelength, a higher sensitivity when using a short excitation wavelength, and, the applicability to samples which are asymmetric with respect to the surface recombination velocity and suggested several promising applications.

[1]D. K. Schroder, *Semiconductor Material and Device Characterization* (John Wiley & Sons, 2006).
[2]H. Steinkemper, M. Hermle, and S. W. Glunz, Prog. Photovoltaics: Res. Appl. **24**, 1319 (2016).
[3]P. Würfel, T. Trupke, T. Puzzer, E. Schäffer, W. Warta, and S. W. Glunz, J. Appl. Phys. **101**, 123110 (2007).
[4]J. A. Giesecke, M. Kasemann, M. C. Schubert, P. Würfel, and W. Warta, Prog. Photovoltaics: Res. Appl. **18**, 10 (2010).
[5]D. Baek, S. Rouvimov, B. Kim, T. C. Jo, and D. K. Schroder, Appl. Phys. Lett. **86**, 112110 (2005).
[6]H. T. Nguyen, Y. Han, M. Ernst, A. Fell, E. Franklin, and D. Macdonald, Appl. Phys. Lett. **107**, 22101 (2015).
[7]B. Michl, J. A. Giesecke, W. Warta, and M. C. Schubert, IEEE J. Photovoltaics **2**, 348 (2012).
[8]K. L. Luke and L.-J. Cheng, J. Appl. Phys. **61**, 2282 (1987).
[9]A. Buczkowski, Z. J. Radzimski, G. A. Rozgonyi, and F. Shimura, J. Appl. Phys. **69**, 6495 (1991).
[10]A. Buczkowski, Z. J. Radzimski, G. A. Rozgonyi, and F. Shimura, J. Appl. Phys. **72**, 2873 (1992); S. Eränen and M. Blomberg, *ibid.* **56**, 2372 (1984); E. Gaubas and J. Vanhellemont, *ibid.* **80**, 6293 (1996); Y. Ogita, *ibid.* **79**, 6954 (1996).
[11]Z. G. Ling and P. K. Ajmera, J. Appl. Phys. **69**, 519 (1991); L. Sirleto, A. Irace, G. F. Vitale, L. Zeni, and A. Cutolo, Opt. Lasers Eng. **38**, 461 (2002); M. Bail and R. Brendel, in Proceedings of the 16th European Photovoltaics Solar Energy Conversion, Glasgow (2000).
[12]G. S. Kousik, Z. G. Ling, and P. K. Ajmera, J. Appl. Phys. **72**, 141 (1992).
[13]Z. G. Ling, P. K. Ajmera, and G. S. Kousik, J. Appl. Phys. **75**, 2718 (1994).
[14]A. J. Sabbah and D. M. Riffe, J. Appl. Phys. **88**, 6954 (2000); O. Palais and A. Arcari, *ibid.* **93**, 4686 (2003).
[15]H.-C. Ostendorf and A. L. Endrös, Appl. Phys. Lett. **71**, 3275 (1997).
[16]B. H. Rose, IEEE Trans. Electron Devices **31**, 559 (1984).
[17]R. Bernini, A. Cutolo, A. Irace, P. Spirito, and L. Zeni, Solid-State Electron. **39**, 1165 (1996).
[18]M. Schöfthaler and R. Brendel, J. Appl. Phys. **77**, 3162 (1995).
[19]F. D. Heinz, J. Giesecke, L. E. Mundt, M. Kasemann, W. Warta, and M. C. Schubert, J. Appl. Phys. **118**, 105706 (2015).
[20]F. Schindler, M. Forster, J. Broisch, J. Schön, J. Giesecke, S. Rein, W. Warta, and M. C. Schubert, Sol. Energy Mater. Sol. Cells **131**, 92 (2014).
[21]C. Schinke, P. Christian Peest, K. Bothe, J. Schmidt, R. Brendel, M. R. Vogt, I. Kröger, S. Winter, A. Schirmacher, S. Lim, H. T. Nguyen, and D. Macdonald, in *5th International Conference on Silicon Photovoltaics, Silicon PV* (2015), Vol. 77, pp. 170.
[22]K. Rühle, M. Rauer, M. Rüdiger, J. Giesecke, T. Niewelt, C. Schmiga, S. W. Glunz, and M. Kasemann, in *Proceedings of the 2nd International Conference on Crystalline Silicon Photovoltaics Silicon PV* (2012), Vol. 27, p. 406.
[23]F. D. Heinz, M. Kasemann, W. Warta, and M. C. Schubert, Appl. Phys. Lett. **107**, 122101 (2015).
[24]J. A. Nelder and R. Mead, Comput. J. **7**, 308 (1965).